Phase transition and elastic constants of zirconium from first-principles calculations

2008 J. Phys.: Condens. Matter 20 235230

(http://iopscience.iop.org/0953-8984/20/23/235230)

IOP Publishing — Journal of Physics: Condensed Matter

J. Phys.: Condens. Matter **20** (2008) 235230 (5pp) doi:10.1088/0953-8984/20/23/235230

Phase transition and elastic constants of zirconium from first-principles calculations

Yan-Jun Hao[1,2], Lin Zhang[2], Xiang-Rong Chen[1,3,4], Ying-Hua Li[2] and Hong-Liang He[2]

[1] School of Physical Science and Technology, Sichuan University, Chengdu 610064, People's Republic of China
[2] Laboratory for Shock Wave and Detonation Physics Research, Institute of Fluid Physics, Chinese Academy of Engineering Physics, PO Box 919-102, Mianyang 621900, People's Republic of China
[3] International Centre for Materials Physics, Chinese Academy of Sciences, Shenyang 110016, People's Republic of China

E-mail: xrchen@126.com

Received 25 November 2007, in final form 14 April 2008
Published 9 May 2008
Online at stacks.iop.org/JPhysCM/20/235230

Abstract
Using the projector augmented wave (PAW) within the Perdew–Burke–Ernzerhof (PBE) form of the generalized gradient approximation (GGA), we investigate the effect of hydrostatic pressure on the structures of zirconium metal at zero temperature. We obtain the $\omega \rightarrow$ bcc transition at around 26.8 GPa, which is in excellent agreement with the experimental values. We also find that the ω phase is most stable at 0 K and 0 GPa. This conclusion is supported by first-principles calculations of Schell *et al* and Jona *et al*. The elastic constants of ω-Zr under high pressures are calculated for the first time. We find that the compressional and shear wave velocities increase monotonically with increasing pressure and the results are in good agreement with the available experimental data. The pressure dependences of three anisotropies of elastic waves are also presented.

1. Introduction

Group IV transition metal zirconium (Zr) and its alloys are very important materials both from scientific and technological points of view. Scientifically, the electronic transfer between the broad sp band and the narrow d band is the driving force behind many structural and electronic transitions in these materials [1–3]. Technologically, these materials have applications in the aerospace industry due to their light weight, static strength and stiffness; they do not degrade rapidly as the temperature increases and they also show oxidation resistance [4]. The mechanical properties of these metals and alloys can be greatly improved by controlling the crystallographic phases present. Pressure is a very important variable in causing phase transformations in this kind of materials.

Static high pressure experimental works indicate that, at room temperature and ambient pressure, Zr is a hexagonal close-packed (hcp) structure (α phase). At high temperature and zero pressure, it transforms martensitically into the body-centered cubic (bcc) structure (β phase) before reaching the melting temperature [5], while at room temperature and under pressure, the hcp phase transforms into another hexagonal structure called the ω phase (AlB_2 type) in the range of 2–7 GPa [6–14]. At further high pressure, 30–35 GPa [7, 12, 15, 16], Zr is observed to transform to the bcc structure.

Shock compression data have also shed light on the high pressure behavior of Zr. Kutsar *et al* [17] observed splitting of a shock wave in Zr, indicating a phase transition occurring at 6.2–6.7 GPa. Song and Gray [18] noted retained ω phase in a Zr sample shocked to 7 GPa, allowing the low pressure transition to be identified as the α–ω transition. McQueen *et al* [19] found anomalies in the Hugoniot at about 26 GPa and indicated phase transitions. Recently, the pressure of the $\alpha \rightarrow \omega$ phase transition for the high purity

[4] Author to whom any correspondence should be addressed.

material was identified as 7.1 GPa by a shock experiment of Cerreta *et al* [20].

Theoretically, the phase transitions of Zr have been the subject of a number of studies using electronic structure [21–25]. They have generally found a transition from $\omega \rightarrow \beta$ at high pressures. However, they found the lowest-energy phase to be not the hcp phase but the ω phase, contrary to experimental observation.

On the other hand, elastic properties of a solid are important because they relate to various fundamental solid-state properties such as interatomic potentials, equation of state, and phonon spectra. Elastic properties are also linked thermodynamically to the specific heat, thermal expansion, Debye temperature, melting point, and Grüneisen parameter. The elastic constants provide valuable information about the bonding characteristic between adjacent atomic planes and the anisotropic character of the bonding and structural stability [26, 27]. Up to now, only a few theoretical methods have been applied successfully to calculate the elastic constants of α-Zr at 0 GPa, such as the full-potential linear-muffin-tin orbital (FP-LMTO) method [28], the ultrasoft pseudopotential method within the generalized gradient approximation (GGA) [29], the tight-binding (TB) approach [30], the embedded-atom (EAM) method [31], and the modified embedded-atom (MEAM) method [32, 33]. However, elastic constants of ω-Zr at high pressures have not yet been reported.

Therefore, in this work we predict the structure phase transition and elastic constants of Zr at high pressures using the projector augmented wave (PAW) method. The predicted elastic constants are used to study the aggregate velocities and elastic anisotropy. We find that the compressional and shear wave velocities increase monotonically with increasing pressure and the results are in good agreement with the available experimental data.

This paper will proceed as follows. In section 2, we make a brief review of the theoretical method. The calculated results with some discussion are presented in section 3. We finish the paper with a summary in section 4.

2. Theoretical methods

2.1. Total energy electronic structure calculations

The electronic structure is calculated self-consistently using the projector augmented wave (PAW) [34, 35] as implemented in the Vienna *ab initio* simulation package (VASP) [36]. For the exchange–correlation potential, the Perdew–Burke–Ernzerhof (PBE) [37] form of the generalized gradient approximation (GGA) is used. In pseudopotential methods, the effect of core electrons and nuclei is replaced by an effective ionic potential, and only the valence electrons, which are directly involved in chemical bonding, are considered. The valence electrons for zirconium are in the $4s^2 4p^6 4d^2 5s^2$ configuration. The Γ-centered grids of k points of $18 \times 18 \times 16$ for α-Zr, $16 \times 16 \times 18$ for ω-Zr and $18 \times 18 \times 18$ for β-Zr are generated according to Monkhorst and Pack [38].

To get accurate results, the plane wave cut-off is set to a high value of 500 eV (18.4 au), which was tested to be fully converged with respect to total energy for many different volumes. A Gaussian smearing for the occupations is used with a smearing width of 0.2 eV. Several test calculations showed the insensitivity of the results with respect to the actual value of this smearing parameter. The optimization of the geometry at each volume is performed via a conjugate-gradient minimization of the free energy, using the Hellmann–Feynman forces on the atoms and stresses on the unit cell. The calculations are converged to 10^{-6} eV/cell and the geometry relaxation is considered to be completed when the total force on the atom is less than 0.02 eV Å^{-1}.

Table 1. The strains used to calculate the elastic constants of hexagonal phase Zr. In the second column, all unlisted elements of strain tensors are set to zero.

Strains	Distortion	$\rho_1 \frac{\partial^2 E(\rho_1,\gamma)}{\partial \gamma^2}\Big\vert_{\gamma=0}$
1	$\varepsilon_{11} = \varepsilon_{33} = \gamma$	$C_{11} + 2C_{13} + C_{33} - 2P$
2	$\varepsilon_{11} = -\varepsilon_{22} = \gamma$	$2(C_{11} - C_{12} - P)$
3	$\varepsilon_{11} = \varepsilon_{22} = \gamma$	$2(C_{11} + C_{12} - P)$
4	$\varepsilon_{13} = \varepsilon_{31} = \gamma$	$4C_{44} - 2P$
5	$\varepsilon_{33} = \gamma$	$C_{33} - P$

2.2. Elastic constants

Based on the theoretical method proposed by Sin'ko and Smirnov [39], we have calculated the elastic constants of c-BN [40] and MgB_2 [41, 42]. Here we give a brief description of this method.

Consider a crystal compressed by the isotropic pressure P to the density $\rho_1 = 1/V_1$ (where V_1 is the distorted volume from the lattice distortion ε_{ij}). Small homogeneous deformation of this crystal takes every Bravais lattice point $\vec{R}'$ of the undistorted lattice to a new position $\vec{R}'$ in the strained lattice

$$R'_i = \sum_j (\delta_{ij} + \varepsilon_{ij}) R_j. \tag{1}$$

For a homogeneous strain, the parameters ε_{ij} are simply constants, independent of $\vec{R}$, where the subscripts i and j indicate the Cartesian components; δ_{ij} is the Kronecker delta. Since a hexagonal crystal structure possesses five independent elastic constants, we thus use the five independent strains listed in table 1. All these strains are non-volume-conserving. The atomic positions are optimized at all strains where they have some degrees of freedom. For each strain, a number of small values of γ are taken to calculate the total energies E for the strained crystal structure. The calculated $E - \gamma$ points are then fitted to the fourth-order polynomial $E(\rho_1, \gamma)$, and the second-order derivatives of $E(\rho_1, \gamma)$ with respect to γ are easily obtained.

3. Results and discussion

3.1. Zero-temperature phase transition

The enthalpy of zirconium's structures relative to that of β phase at high pressures is presented in figure 1 at zero temperature. From this figure, we find the following.

Table 2. The lattice constants (Å), bulk modulus (GPa) and its pressure derivative of Zr at zero pressure and zero temperature, compared with the experimental data and other theoretical results. (Italic numbers indicate values being fixed.)

		This work	Other calculations	Experiments
α	a	3.240	3.232 [48], 3.231 [31], 3.202 [46], 3.232 [47]	3.231 [9]
	c	5.178	5.182 [48], 5.125 [31], 5.218 [46], 5.147 [47]	5.148 [9]
	B_0	93.4	97.1 [31], 99.8 [46], 97.5 [47]	97.6 [9], 94 [11]
	B_0'	3.22		3.10 [11]
ω	a	5.056	5.050 [48]	5.039 [44]
	c	3.150	3.150 [48]	3.150 [44]
	B_0	101.1		90.0 [11], 109.0 [11], 104.0 [7, 14]
	B_0'	3.27		*4.0* [11], *2.05* [7, 11]
β	a	3.580	3.577 [48], 3.580 [31]	3.574 [45]

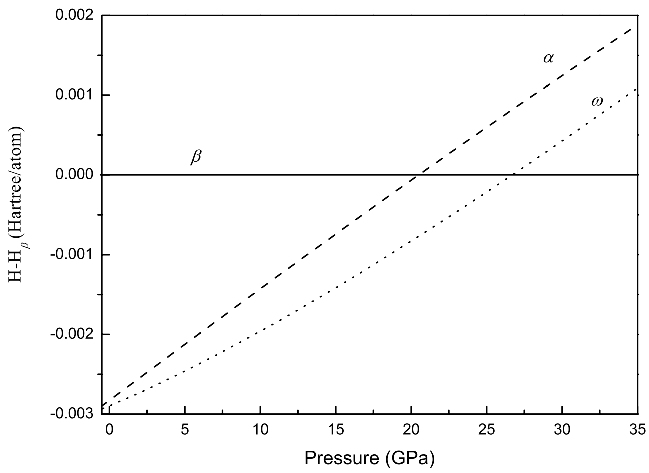

Figure 1. Enthalpy variation as a function of pressure for α and ω, relative to that of β phase. The enthalpy of the β structure is taken as a reference level.

(1) ω-Zr is most stable at 0 GPa. This conclusion is supported by first-principles calculations of Schell *et al* [23, 24] and is apparently inconsistent with experiment values. This obvious contradiction is because our calculation is valid only at 0 K, while the experimental result is obtained from room temperature. The disagreement between the theory and the experiment is likely due to the thermal effect.

(2) The $\alpha \rightarrow \beta$ phase transitions occur at about 20.5 GPa; moreover, when $P < 20.5$ GPa, ω-Zr is still more stable than the other two.

(3) The calculated ω to β phase transition pressure is 26.8 GPa, which is in excellent agreement with experimental data [7, 12, 15, 16, 19] and the full-potential linearized augmented plane wave (FP-LAPW) results of 28.2 GPa [24] and 27 GPa [25].

3.2. Elastic constants and elastic anisotropy at zero temperature

The equilibrium lattice parameters, bulk modulus and its pressure derivative are obtained by calculating the electronic static free energy and pressure for different unit cell volumes and by fitting the calculated data to the Vinet equation of state (EOS) [43]. The calculated equilibrium lattice parameters, the bulk modulus and its pressure derivative are displayed in table 2, along with experimental measurements [9, 44, 45] and other theoretical results [31, 46–48]. It is seen that the calculated lattice parameters agree with experiments and other theoretical calculations to a fraction of one per cent. The bulk modulus and its pressure derivative are also in excellent agreement with other available theoretical results and experimental data.

Table 3. The elastic constants C_{ij} in GPa of α-Zr at $T = 0$ K and $P = 0$ GPa, along with other theoretical values and experiments. Here $C_{66} = (C_{11} - C_{12})/2$.

Elastic constants	C_{11}	C_{12}	C_{13}	C_{33}	C_{44}	C_{66}
α-Zr	141.1	67.6	64.3	166.9	25.8	36.8
FP-LMTO [28]	153.1	63.4	76.5	171.2	22.4	44.9
DFT [29]	139.4	71.3	66.3	162.7	25.5	34.1
TB [30]	142.0	71.0	71.0	147.0	8.0	35.5
EAM [31]	147.9	66.3	66.2	182.7	39.2	40.8
MEAM [32]	151.5	71.8	66.1	160.6	34.1	39.9
MEAM [33]	152.0	74.0	63.2	153.3	33.2	39.0
Experiments [49]	144.0	74.0	67.0	166.0	33.0	35.0

Table 4. The elastic constants C_{ij} in GPa of ω-Zr at different pressures and zero temperature.

P	C_{11}	C_{12}	C_{13}	C_{33}	C_{44}
0	165.2	75.6	47.5	198.7	30.6
6	202.0	85.1	56.8	235.2	39.6
10	221.1	90.6	60.8	257.4	43.3
15	251.7	103.6	65.9	287.4	47.3
20	275.1	119.4	69.0	298.4	48.8

In table 3, we list the calculated elastic constants of α-Zr, compared with experimental data and the previous calculations. Obviously, our results are in accordance with the experimental values [46] and results calculated by others [28, 29, 31–33] except for those by Schnell *et al* [30].

The calculated pressure dependences of the elastic constants of ω-Zr at zero temperature are shown in table 4. It is found that the five elastic constants increase monotonically with the applied pressure. C_{11} and C_{33} increase quickly with the increasing pressure, and C_{13} has a moderate increase as well as C_{12} and C_{44}. The elastic constants C_{11} and C_{33} are important, because they are related to the deformation behavior and atomic bonding characteristics of the transition metal. It can be seen from table 4 that $C_{33} > C_{11}$ for ω-Zr. The

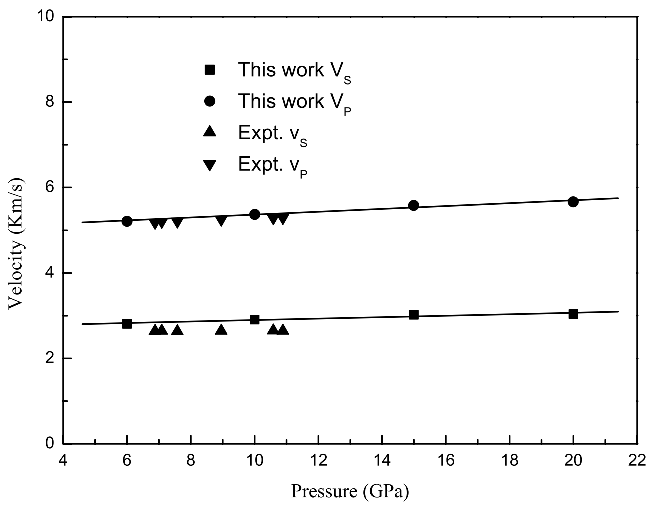

Figure 2. Predicted compressional and shear wave velocities of ω-Zr as a function of pressure. The solid triangles are experimental data of Liu *et al* [14].

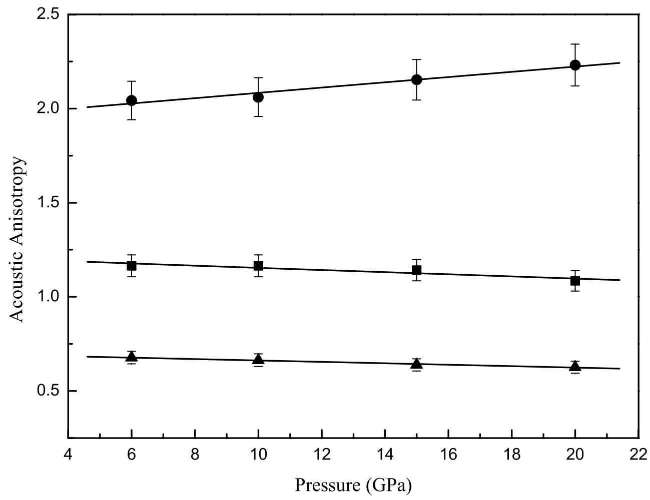

Figure 3. Anisotropies (Δ_P (compressional wave), Δ_{S1} and Δ_{S2} (shear waves)) of ω-Zr as a function of pressure P. The solid squares, solid circles and solid triangles with error bars represent Δ_P, Δ_{S1} and Δ_{S2}, respectively.

implication of this is that the atomic bonds along the {001} planes between nearest neighbors are stronger than those along the {100} plane.

From elastic constants, we can obtain the bulk modulus B and shear modulus G according to the Voigt–Reuss–Hill (VRH) average scheme [50]. Thus, the isotropically averaged aggregate velocities for compressional (v_P) and shear waves (v_S) are expressed as [51]

$$v_p = \sqrt{(B + \tfrac{4}{3}G)/\rho}, \qquad v_s = \sqrt{G/\rho} \tag{2}$$

with ρ the density. The obtained compressional and shear wave velocities are predicted in figure 2. It is noted that v_P and v_S increase monotonically with increasing pressure. The compressional wave velocities are in good agreement with the experimental data of Liu *et al* [14] and the shear wave velocities are slightly overestimated in comparison with the experimental values of Liu *et al* [14], but the whole trend is in agreement with them.

The acoustic velocities are related to the elastic constants by the Christoffel equation

$$(C_{ijkl}n_j n_k - \rho v^2 \delta_{il})u_i = 0 \tag{3}$$

where C_{ijkl} is the fourth rank tensor description of elastic constants, $\mathbf{n}$ is the propagation direction, ρ is the density, $\mathbf{u}$ the polarization vector, $M = \rho v^2$ is the modulus of propagation and v the velocity. The acoustic anisotropy can be described as

$$\Delta_i = \frac{M_i\,[n_x]}{M_i\,[100]}, \tag{4}$$

where n_x is the extremal propagation direction other than [100] and i is the three types of elastic wave index (one longitudinal and two polarizations of the shear wave). By solving equation (3) for ω-Zr, one can obtain the anisotropy of the compressional wave (P)

$$\Delta_P = \frac{C_{33}}{C_{11}}. \tag{5}$$

The anisotropies of the wave polarized perpendicular to the basal plane ($S1$) and the polarized one in the basal plane ($S2$) are written as

$$\Delta_{S1} = \frac{C_{11} + C_{33} - 2C_{13}}{4C_{44}} \tag{6}$$

$$\Delta_{S2} = \frac{2C_{44}}{C_{11} - C_{12}}. \tag{7}$$

While for $S2$ and P waves the extremum occurs along the c axis, for $S1$ it is at an angle of 45° from the c axis in the a–c plane. We note that an additional extremum may occur for the compressional wave propagation at intermediate directions depending on the values of the elastic constants.

Figure 3 presents the obtained pressure dependences of three anisotropies of elastic waves. It is found that Δ_P and Δ_{S2} descend slightly as pressure increases, while Δ_{S1} ascends as pressure rises. These results can be understood by comparison to an hcp crystal interacting with central nearest-neighbor forces (CNNF) [52]. For this model the elastic anisotropy is independent of the interatomic potential to lowest order in P/C_{11}, hence the anisotropy is dependent on the symmetry of the crystal only. We also noted that the value of Δ_P has the tendency to approach 1.0 gradually, while the values of Δ_{S1} and Δ_{S2} go away from 1.0. This means that the anisotropies of the wave polarized perpendicular to the basal plane ($S1$) and the wave polarized in the basal plane ($S2$) become strong, but the anisotropy of the compressional elastic wave (P) will gradually weaken with the pressure increasing. These results indicate that the axial ratio c/a decreases with the pressure rising and the anisotropy of the bonding between one Zr atom and its neighbor Zr atoms from different directions will be weakened.

4. Conclusion

In summary, we investigate the phase transitions of metal Zr and find that ω-Zr is most stable at 0 GPa and the $\omega \rightarrow \beta$

transition pressure at $T = 0$ is 26.8 GPa, which is a little lower compared with experiments. The most likely cause for this discrepancy is because small amounts of impurities suppress the experimental phase transition The elastic constants of α-Zr at $T = 0$ and $P = 0$ are in good agreement with experimental results and previous calculations. The elastic constants of ω-Zr under high pressures are predicted for the first time. The isotropically averaged aggregate velocities increase monotonically with increasing pressure. The pressure dependences of three anisotropies of elastic waves are also predicted.

Acknowledgments

We acknowledge the support for this work by the National Natural Science Foundation of China under grants No 10476027 and No 10576020 and the NSAF under grant No 10776022.

References

[1] Gyanchandani J, Gupta S, Sikka S and Chidambaram R 1990 *J. Phys.: Condens. Matter* **2** 6457
[2] Gyanchandani J, Gupta S, Sikka S and Chidambaram R 1990 *J. Phys.: Condens. Matter* **2** 301
[3] Kutepov A L and Kutepova S G 2003 *Phys. Rev.* B **67** 132102
[4] Ahuja R, Dubrovinsky L, Dubrovinskaia N, Osorio Guillen J M, Mattesini M, Johansson B and Le Bihan T 2004 *Phys. Rev.* B **69** 184102
[5] Young D A 1991 *Phase Diagrams of the Elements* (Berkeley, CA: University of California Press)
[6] Sikka S K, Vohra Y K and Chidambaram R 1982 *Prog. Mater. Sci.* **27** 245
[7] Xia H, Duclos S J, Ruoff A L and Vohra Y K 1990 *Phys. Rev. Lett.* **64** 204
[8] Donohue J 1974 *The Structures of the Elements* (New York: Wiley)
[9] Olinger B and Jamieson J C 1973 *High Temp. High Pressures* **5** 123
[10] Jamieson J C 1963 *Science* **140** 72
[11] Zhao Y S *et al* 2005 *Phys. Rev.* B **71** 184119
[12] Akahama Y, Kobayashi M and Kawamura H 1991 *J. Phys. Soc. Japan* **60** 3211
[13] Zhang J Z *et al* 2005 *J. Phys. Chem. Solids* **66** 1213
[14] Liu W, Li B S, Wang L P, Zhang J Z and Zhao Y S 2007 *Phys. Rev.* B **76** 144107
[15] Bridgman P W 1952 *Proc. Am. Acad. Arts Sci.* **81** 165
[16] Xia H, Ruoff A L and Vohra Y K 1991 *Phys. Rev.* B **44** 10374
[17] Kutsar A R, Pavlovskii M N and Kamissarov V V 1984 *JETP Lett.* **39** 480
[18] Song S G and Gray III G T 1995 *Phil. Mag.* A **71** 275
[19] McQueen R G, Marsh S P, Taylor J W, Fritz J N and Carter W J 1970 *High Velocity Impact Phenomena* ed R Kinslow (New York: Academic)
[20] Cerreta E, Gray III G T, Hixson R S, Rigg P A and Brown D W 2005 *Acta Mater.* **53** 1758
[21] Jyoti G and Gupta S C 1994 *J. Phys.: Condens. Matter* **6** 10273
[22] Ostanin S A and Trubitsin V Y 1998 *Phys. Rev.* B **57** 13485
[23] Jona F and Marcus P M 2003 *J. Phys.: Condens. Matter* **15** 5009
[24] Schnell I and Albers R C 2006 *J. Phys.: Condens. Matter* **18** 1483
[25] Joshi K D, Jyoti G, Gupta S C and Sikka S K 2002 *J. Phys.: Condens. Matter* **14** 10921
[26] Ravindran P, Fast Lars, Korzhavyi P A, Johansson B, Wills J M and Eriksson O 1998 *J. Appl. Phys.* **84** 4891
[27] Louail L, Maouche D, Roumili A and Ali Sahraoui F 2004 *Mater. Lett.* **58** 2975
[28] Clouet E, Sanchez J M and Sigli C 2002 *Phys. Rev.* B **65** 094105
[29] Ikehata H, Nagasako N, Furuta T, Fukumoto A, Miwa K and Saito T 2004 *Phys. Rev.* B **70** 174113
[30] Schnell I, Jones M D, Rudin S P and Albers R C 2006 *Phys. Rev.* B **74** 054104
[31] Oh D J and Johnson R A 1989 *J. Nucl. Mater.* **169** 5
[32] Kim Y M, Lee B J and Baskes M I 2006 *Phys. Rev.* B **74** 014101
[33] Baskes M I and Johnson R A 1994 *Modelling Simul. Mater. Sci. Eng.* **2** 147
[34] Blöchl P E 1994 *Phys. Rev.* B **50** 17953
[35] Kresse G and Joubert J 1999 *Phys. Rev.* B **59** 1758
[36] Kresse G and Furthmüller J 1996 *Phys. Rev.* B **54** 11169
[37] Perdew J P, Chevary J A, Vosko S H, Jackson K A, Pederson M R, Singh D J and Fiolhais C 1992 *Phys. Rev.* B **46** 6671
[38] Monkhorst H J and Pack J D 1976 *Phys. Rev.* **B 13** 5188
[39] Sin'ko G V and Smirnov N A 2002 *J. Phys.: Condens. Matter* **14** 6989
[40] Hao Y J, Chen X R, Cui H L and Bai Y L 2006 *Physica* B **382** 118
[41] Wang H Y, Chen X R, Zhu W J and Cheng Y 2005 *Phys. Rev.* B **72** 172502
[42] Guo H Z, Chen X R, Zhu J, Cai L C and Gao J 2005 *Chin. Phys. Lett.* **22** 1764
[43] Vinet P, Rose J H, Ferrante J and Smith J R 1989 *J. Phys.: Condens. Matter* **1** 1941
[44] Barrett C S and Massalski T B 1966 *Structure of Metals* (New York: McGraw-Hill)
[45] Heiming A, Petry W, Trampenau J, Alba M, Herzig C, Schober H R and Vogl G 1991 *Phys. Rev.* B **43** 10948
[46] Willaime F and Massobrio C 1991 *Phys. Rev.* B **43** 11653
[47] Cleri F and Rosato V 1993 *Phys. Rev.* B **48** 22
[48] Greeff C W 2005 *Modelling Simul. Mater. Sci. Eng.* **13** 1015
[49] Brandes E A 1983 *Smithells Metals Reference Book* (London: Butterworth)
[50] Hill R 1952 *Proc. Phys. Soc. London* **65** 350
[51] Schreiber E, Anderson O L and Soga N 1973 *Elastic Constants and their Measurements* (New York: McGraw-Hill)
[52] Born M and Huang K 1954 *Dynamical Theory of Crystal Lattices* (Oxford: Clarendon)